Mutation at Expanding Front of Self-Replicating Colloidal Clusters

Hidenori Tanaka, Zorana Zeravcic, and Michael P. Brenner

Phys. Rev. Lett. **117**, 238004 — Published 2 December 2016

DOI: 10.1103/PhysRevLett.117.238004

Mutation at Expanding Front of Self-Replicating Colloidal Clusters

Hidenori Tanaka,[1,2,*] Zorana Zeravcic,[1,3] and Michael P. Brenner[1,2]

[1] *Harvard John A. Paulson School of Engineering and Applied Sciences, Harvard University, Cambridge, MA 02138*
[2] *Kavli Institute for Bionano Science and Technology, Harvard University, Cambridge, MA 02138*
[3] *Soft matter and chemistry laboratory, ESPCI PSL Research University, 75005 Paris, France*

(Dated: November 15, 2016)

We construct a scheme for self-replicating square clusters of particles in two spatial dimensions, and validate it with computer simulations in a finite-temperature heat bath. We find that the self-replication reactions propagate through the bath in the form of Fisher waves. Our model reflects existing colloidal systems, but is simple enough to allow simulation of many generations and thereby the first study of evolutionary dynamics in an artificial system. By introducing spatially localized mutations in the replication rules, we show that the mutated cluster population can survive and spread with the expanding front in circular sectors of the colony.

PACS numbers: 81.05.Zx, 81.16.Dn, 87.23.Cc, 82.70.Dd

Self-replication followed by mutation and evolution is a key driver of biological complexity. The change of fitness landscapes due to environmental conditions creates the driving force for the evolution of new functionalities. A holy grail of modern materials science research is to emulate this natural evolution of functionality, and to design materials systems where evolution based discovery strategies could apply. Creating a population dynamics in materials requires both designing efficient self-replication, as well as some mechanism for mutating the dynamics so that novel structures can arise.

Recently, initial steps towards creating self-replicating artificial materials have been taken using DNA nanotechnology [1–4], light switchable colloidal dimers [5] or magnetic dipolar colloids [6]. With DNA based interactions, hybridization causes specific, short range interactions between nano/micro scale components, and both the specificity [7, 8] and the timescales [9] of the interactions between strands can be chosen by tuning the DNA sequences. A striking study [2] uses chains of DNA tiles as templates for replication, achieving a few generations of replication in experiments. More recently, these ideas were extended to ring structures [4] of DNA tile motifs. A theoretical study [10] demonstrated how specific interactions can lead to self-replication of finite clusters of particles.

Up until now, there has been no explicit demonstration of mutation/amplification cycles in a self-replicating material, either theoretically or experimentally. A major challenge has been the difficulty in either experiments or simulations of producing enough replication cycles that a meaningful mutation could be carried out. In contrast, selected evolution of DNA or RNA is a common technology due to the highly efficient and optimized Polymerase Chain Reaction [11]. In this paper, we introduce a model of self-replicating clusters that is computationally tractable enough that we can explicitly study the emergence of mutations. We demonstrate a phenomenology that is strikingly similar to the development of mutations in growing bacterial colonies [12–14].

Our system consists of colloids confined to two dimensions. The self-replicating objects are colloidal clusters that make their progeny through a geometrical templating scheme introduced earlier [10]. Our model is directly related to recent experiments on clusters of identical colloidal particles [15]. To allow the complexity of self-replication and mutation/selection phenomena, we model colloids coated with specific DNA strands such as ones already realized in self-assembly experiments [16–22]. The fact that the system is two dimensional gives substantial computational savings, making it possible to simulate large systems with > 20 generations (see SI section I [23] for the definition) of progeny.

We find two striking features of our model of self-replicating clusters: First, when the clusters grow exponentially, they deplete monomers from the bath causing the formation of a propagating front obeying Fisher's dynamics [24, 25]. Second, a single cluster with a changed replication rule ("mutation") can initiate a population change within the expanding front and form a sector of mutated structures ("genetic drift"). As we will argue below, we believe our model presents the first observation of evolutionary dynamics in a controlled artificial self-replicating system.

In our system, the surface of each colloid is covered by DNA strands which mediate specific short range attraction between pairs of particles. We choose to consider replication of square clusters, as a simple example that is not constrained to a linear geometry. When each particle in the parent cluster can attach at most one complementary monomer, geometrical constraints prevent direct templating from a single parent. Inspired by previous work [10], we circumvent this problem by templating a square cluster between two parent square clusters, Fig. 1(a). The self-replication scheme begins when two parent square clusters, each composed of A, B particle species (stage I), each attach complementary particles, species A', B', respectively, from the monomer

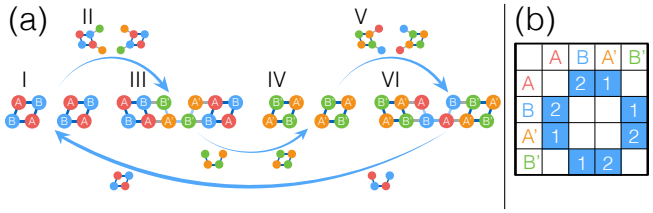

FIG. 1. (a) Self-replication scheme of square clusters with $n_c = 3$. The reaction starts with two square clusters composed of A and B particle species, having permanent bonds (stage I). Complementary monomers (A',B') attach to the clusters (stage II) and attraction among the attached monomers leads to templating of another 4-mer structure (stage III). The thus formed complementary cluster templates a new cluster in the same way, thereby closing the hypercycle (stages IV to VI). (b) Interaction matrix of particle species. Blue matrix entries represent attractive interaction, and white entries represent repulsive force, while the inscribed number specifies the species valence.

bath (see Fig. 1(b)), thereby forming two independent hairy squares (stage II). Then, attraction between A' and B' allows bonding of the two hairy clusters (stage III). The formed structure of complementary particles is detached from the parents (stage IV), forming a square. The square made of A',B' particles now becomes a parent involved in templating its complementary (A,B) square thus closing the hypercycle (stages V, VI).

The detachment step between stages III and IV (Fig. 1(a)) is critical in self-replication reactions [26]. In our simulations, we model the detachment process as in Ref.[10]: When the number of bonds n between attached monomers (while they are attached to their respective parents) reaches the critical value n_c, the bonds between parent particles and monomers are removed and the existing bonds between the monomers become irreversible (see SI section II [23]). In practice, n can increase by more than one within a single simulation timestep. Therefore, for a chosen n_c, a newly formed structure can have $n \geq n_c$ and a non-square geometry, and can become a parent for future reactions that can significantly deviate from the scheme in Fig. 1(a).

To investigate emergent behavior in this system, we perform Brownian dynamics simulations. The dynamics of the i-th particle is governed by the over-damped Langevin equation

$$\partial_t \boldsymbol{r}_i = -\mu \sum_{j \neq i} \boldsymbol{\nabla} U(r_{ij}) + \boldsymbol{\eta}_i(t), \qquad (1)$$

where $\boldsymbol{r}_i$ is its position vector, $r_{ij} \equiv |\boldsymbol{r}_i - \boldsymbol{r}_j|$, and μ is the mobility. The short range interaction between i-th and j-th particle $U(r_{ij})$ is given by a modified Morse potential in case of attraction, and harmonic potential in case of repulsion (see SI section III [23]). The interaction range is $1.05d$ in case of attraction and $1.0d$ in case of repulsion, where d is the particle diameter. The implementation of short ranged interactions is validated against recent experimental results on colloidal clusters in $2d$ [15] (see SI section IV [23]). The noise term $\boldsymbol{\eta}_i(t)$ satisfies the fluctuation-dissipation relation $\langle \eta_{i\alpha}(t)\eta_{j\beta}(t')\rangle = 2D\delta_{ij}\delta_{\alpha\beta}\delta(t-t')$ where $\alpha, \beta = x, y$, and D is the diffusion constant of monomers. In our simulation, we measure length in units of particle diameter d, time in d^2/D, energy in k_BT.

We simulate a system of $N = 1652$ particles with an area fraction $\phi = 0.193$ in a square box ($L = 82d$) with periodic boundary conditions, and we keep the tempera-

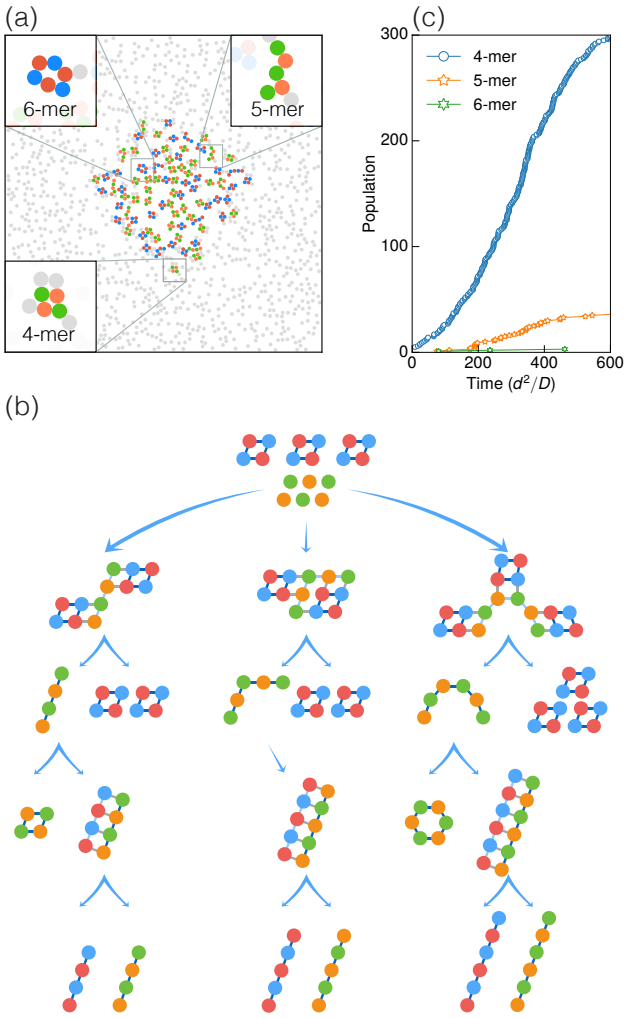

FIG. 2. Brownian dynamics simulation of self-replicating colloidal clusters using 1652 colloidal particles. (a) A snapshot from our simulation: Particles are colored according to their species (Fig. 1(a)) if they comprise a cluster; otherwise they are gray. This snapshot shows successful replication of desired 4-mer (square) cluster as well as other undesired 5-mer and 6-mer structures. (b) Example of frequent replication pathways leading to formation of each of the 4-, 5- and 6-mers. (c) Population of 4-mers, 5-mers and 6-mers as a function of time.

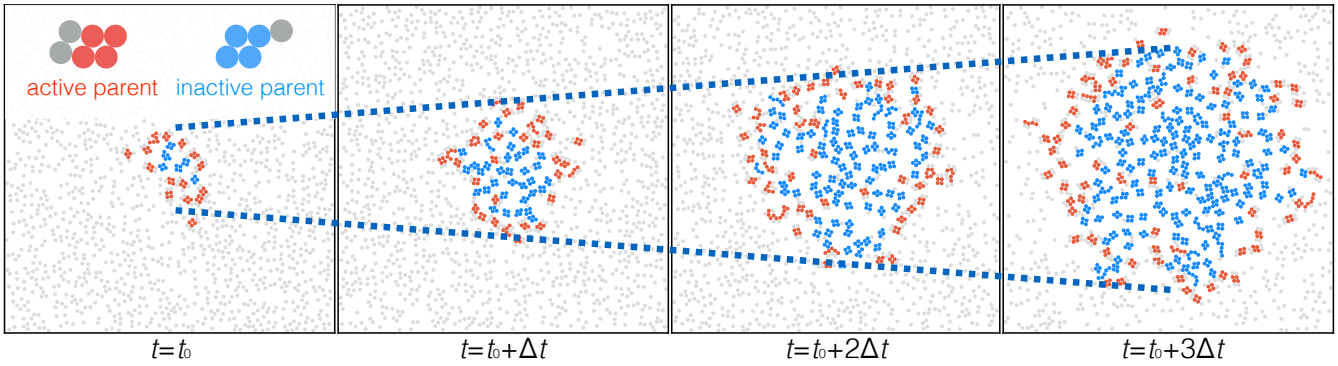

FIG. 3. Simulation snapshots taken at $\Delta t = 100d^2/D$ intervals. Clusters with at least two attached monomers are colored red (active parents) and clusters with less than two attached monomers are colored blue (inactive parents). Dashed lines ($\propto t$) are guides to the eye.

ture fixed. Sixteen out of N particles comprise four initial parent square clusters placed around the center. We set $n_c = 3$, so that detachment reaction occurs when at least three bonds form between attached monomers. To simplify simulations, we do not allow the free monomers to interact with each other. Fig. 2(a) shows a typical snapshot from our simulation. As clusters replicate and diffuse, they form a circular colony. The colony mainly contains our designed structure, the square, but we also find geometrically distinct structures of 4, 5 or 6 particles, whose formation is allowed by the detachment criterion $n_c = 3$. Since there is no attraction between particles of the same species (Fig. 1(b)), 5-mers can only exist as chains while 4- and 6-mers only form squares and hexagons, respectively (see insets of panel Fig. 2 (a)). Examples of frequently observed replication pathways of these structures are shown in Fig. 2(b) (see SI section V [23]). Fig. 2(c) shows the time dependence of the population of each of these structures, demonstrating that with $n_c = 3$ the square clusters dominate.

Using our observation of self-replication over generations we analyze properties of spatiotemporal structure of the colony. Fig. 3 illustrates the spatial distribution of replication reactions. We find that a good indicator [27] of where the replication happens is the location of parents with at least two attached monomers, and we label such parents "active" (colored red). Most of the active parents localize in a thin band at the boundary of the colony, whereas most of the clusters in the interior are "inactive" (colored blue).

To understand the spatial spreading of the colony, we consider the time evolution of a coarse-grained population density field of clusters $u(\boldsymbol{r}, t)$ through a Fisher-Kolmogorov-Petrovskii-Piskunov (F-KPP) type of reaction-diffusion equation [24, 25]:

$$\frac{\partial u}{\partial t} = \alpha u(1-u) + D_{\rm eff}\nabla^2 u, \tag{2}$$

with initial growth rate α, and an effective diffusion constant $D_{\rm eff}$. This equation has an asymptotic traveling wave solution of circular symmetry $u(r,t) = f(r - v_{\rm front}t)$, where the front velocity

$$v_{\rm front} = 2\sqrt{D_{\rm eff}\alpha} \tag{3}$$

at large r [28, 29]. Fig. 4(a) shows that the colony radius moves at constant velocity, measured to be $v_{\rm front} = 0.08D/d$. We also directly measure the initial growth rate of the colony to be $\alpha = 1.5 \times 10^{-2} D/d^2$, giving the estimate $D_{\rm eff} \approx 0.11D$ from Eq. (3). To validate the F-KPP dynamics entailed by Eq. (3), from our simulations we directly measure the effective diffusion constant of all clusters, $D_{\rm eff}^{\rm sim}$, which takes into account that clusters are found in different stages of self-replication reaction, Fig. 1 (a) (see SI section VI [23]). We find $D_{\rm eff}^{\rm sim} = 0.12 \pm 0.04D$, in good agreement with the estimated $D_{\rm eff}$.

The F-KPP dynamics implies a length scale

$$\lambda = \sqrt{D_{\rm eff}/\alpha} \tag{4}$$

which sets the width of the traveling front (Fisher wave), estimated here to be $\lambda = 3d$. When the system size L is much less than λ, one can only observe an exponential growth of the colony without formation of a front. In the opposite regime $\lambda \ll L$ one observes an initial exponential growth followed by formation of a propagating front and growth of colony as a power-law t^d with d the spatial dimension. Our simulations are in the latter regime, exhibiting the propagation of fully-formed front whose estimated width of order $\lambda = 3d$ is consistent with the width of region populated by active parents in Fig. 3 (see SI section VII [23]). In Fig. 4(b) we show the colony size, i.e., the total population of all clusters over time, averaged over 10 independent simulations. The growth curve is quadratic in time (after initial exponential expansion) as expected from F-KPP dynamics. An intuitive explanation of this power-law follows from assuming that the

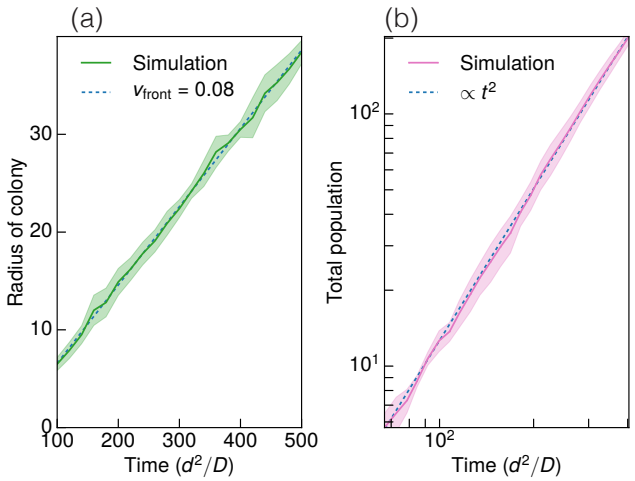

FIG. 4. (a) Log-log plot of the total population as a function of time. The solid line is the average over 10 independent simulations. The shaded region shows one standard deviation above and below the average, while the dashed line ($\propto t^2$) is the best linear fit. (b) Radius of the circular colony as function of time. The solid line is the average over 10 independent simulations. The shaded region shows one standard deviation above and below the average. The dashed line is the best linear fit, suggesting emergence of expanding front with constant velocity.

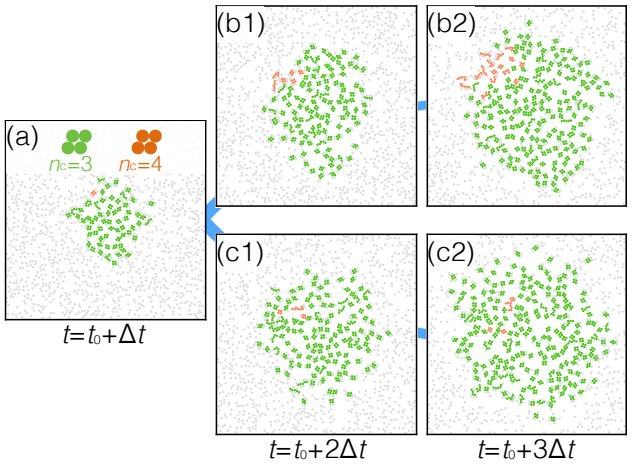

FIG. 5. (a) The second snapshot ($t = t_0 + \Delta t$) of Fig. 3 is shown, where one square cluster (orange) at the boundary is mutated by assigning it $n_c = 4$. All other clusters (green) retain $n_c = 3$. (b1-b2) and (c1-c2) are results from two independent simulations started from (a). The mutated progeny either dominates in a circular sector of the colony (b1) and survives with expanding front (b2); or stays within the colony bulk (c1) and stops reproducing (c2).

replication process occurs within the front which has a constant width. Then the number of newly created clusters per unit time at time t is proportional to $\sqrt{N_{\text{clust}}(t)}$, which leads to the quadratic population growth.

Finally, we consider mutations in the cluster population. We seek to define a "mutation" as a hereditary trait that leads to altered properties. Within our model, the size and shape of a parent will not persist through many generations of progeny (see Fig. 2(b)). We can however define a mutation as a change of the replication rule $n_c = 3$ into $n_c = 4$: First, this property can be inherited by every daughter of the mutated cluster (a dominant trait); second, a mutated population has a strikingly different distribution of cluster sizes than the non-mutated population. In particular, $n_c = 3$ population is majority 4-mers with only $\sim$ 10% of 5-mers (see Fig. 2(c) and S2(a)), while mutated population with $n_c = 4$ has $\sim$ 70% of 5-mers (see Fig. S2(b)). To investigate mutations, we start from the colony in the second panel of Fig. 3, and select a single square cluster at the edge of colony, Fig. 5(a). We mutate this cluster, leaving all others intact. Fig. 5 shows two different outcomes of 13 simulations started with this initial condition: In panels (b1-b2), the population of mutated structures grows at the expanding front and dominates in a circular sector. As expected, the population in the sector is majority 5-mers. In contrast, in panels (c1-c2) the mutation goes extinct, since the progeny of the mutated cluster stops reproducing in the monomer-deficient colony bulk.

To judge how mutation affects the "fitness" of population, in each simulation we trace the progeny of the mutated cluster and the progeny of several randomly selected non-mutated clusters at the opposite side of the colony front. The outcomes indicate that the survival probability for the mutated lineage is lower ($62\% \pm 15\%$) than for the non-mutated ($83\% \pm 11\%$) (for details see SI section VIII [23]). We relate the lowered fitness of mutated population to the fact that the mutated clusters on average need to consume more monomers compared to their non-mutated competitors on the front. The competitive advantage can be observed by comparing a purely non-mutated and a purely mutated colony: The rate of monomer consumption is similar (Fig. S6(b)), while the growth rate of the mutated colony lags behind (Fig. S6(c)) as described in SI section VIII. The fact that survival of a (non-)mutated cluster lineage is subject to randomness by definition entails "genetic drift". In our system we directly observe the genetic drift because lineages propagate spatially with the Fisher's wave.

In summary, we have introduced a model of self-replicating colloidal clusters which despite its simplicity shows remarkably rich behavior including Fisher wave propagation, and the possibility of studying mutations, fitness and genetic drift, as some of key components of evolutionary dynamics. Very recently, propagating reaction-diffusion fronts have been observed in different synthetic self-replicating systems at the molecular scale [30, 31]. Our system relates to an artificial material at

the mesoscale. We remark that the basic ingredients required to experimentally realize our system are becoming available. Controlled valence of isotropic mesoscale particles has been demonstrated [7, 32]. We believe that the detachment step could be realized with time-dependent interactions that can either strengthen (among attached monomers) or weaken (between the parent cluster and attached monomers) in time [33], which require consumption of energy. A first step towards time-dependent interactions has been realized between nanoparticles using complex strand-displacement reactions that rely on a DNA fuel source [9, 34]. An alternative is to globally cycle temperature and light to achieve the detachment process and cluster stabilization, a strategy already used in some studies [1, 2]. The final ingredient — implementation of the mutation mechanism — is still an open problem. We require a change in the characteristic time of the detachment process, therefore changing which structure is preferred by the replication process. At the same time, this change in the replication process needs to be inherited by daughters. Although a specific mechanism for this is unclear at the moment, we believe the flexibility provided by the DNA nanotechnology is sufficient to realize it. Our concept is, however, applicable to artificial systems at different scales and opens a new door for implementing evolutionary dynamics in experiments.

H.T. would like to thank H. Isobe, K. Kawaguchi, A.A. Lee and members of Manoharan lab for fruitful discussions. H.T. is supported by the Funai Foundation for Information Technology through Funai Overseas Scholarship. The computations in this paper were run on the Odyssey cluster supported by the FAS Division of Science, Research Computing Group at Harvard University. This research was funded by the NSF grant DMR-1435964, the Harvard MRSEC grant DMR1420570, and the Division of Mathematical Sciences Grant DMS-1411694. M.P.B. is an investigator of the Simons Foundation.

* tanaka@g.harvard.edu

[1] M. E. Leunissen, R. Dreyfus, N. C. Seeman, D. J. Pine, and P. M. Chaikin, Soft Matter (2009).
[2] T. Wang, R. Sha, R. Dreyfus, M. E. Leunissen, C. Maass, and et al., Nature **478** (2011).
[3] R. Schulman, B. Yurke, and E. Winfree, Proceedings of the National Academy of Sciences **109**, 6405 (2012).
[4] J. Kim, J. Lee, S. Hamada, S. Murata, and S. H. Park, Nature nanotechnology **10**, 528 (2015).
[5] R. Zhang, D. A. Walker, B. A. Grzybowski, and M. Olvera de la Cruz, Angew. Chem. **126**, 177 (2014).
[6] J. M. Dempster, R. Zhang, and M. Olvera de la Cruz, Phys. Rev. E **92**, 042305 (2015).
[7] L. Feng, L.-L. Pontani, R. Dreyfus, P. Chaikin, and J. Brujic, Soft Matter **9**, 9816 (2013).
[8] M. E. Leunissen, R. e. m. Dreyfus, F. C. Cheong, D. G. Grier, R. Sha, N. C. Seeman, and P. M. Chaikin, Nature Materials **8**, 590 (2009).
[9] A. J. Turberfield, B. Yurke, A. P. Mills, F. C. Simmel, and J. L. Neumann, Nature **406**, 605 (2000).
[10] Z. Zeravcic and M. P. Brenner, Proc. Natl. Acad. Sci. **111**, 1748 (2014).
[11] M. A. Innis, D. H. Gelfand, J. J. Sninsky, and T. J. White, *PCR protocols: a guide to methods and applications* (Academic press, 2012).
[12] S. R. Hallatschek Oskar, Pascal Hersen and D. R. Nelson, Proc. Natl. Acad. Sci. , 104 (2007).
[13] K. S. Korolev, M. Avlund, O. Hallatschek, and D. R. Nelson, Reviews of modern physics **82**, 1691 (2010).
[14] K. S. Korolev, J. B. Xavier, D. R. Nelson, and K. R. Foster, The American Naturalist **178**, 538 (2011).
[15] R. W. Perry, M. C. Holmes-Cerfon, M. P. Brenner, and V. N. Manoharan, Phys. rev. lett. **114**, 228301 (2015).
[16] M. R. Jones, N. C. Seeman, and C. A. Mirkin, Science (2015).
[17] K.-T. Wu, L. Feng, R. Sha, R. Dreyfus, A. Y. Grosberg, N. C. Seeman, and P. M. Chaikin, Physical Review E **88**, 022304 (2013).
[18] W. B. Rogers and V. N. Manoharan, Science **347**, 639 (2015).
[19] W. B. Rogers and J. C. Crocker, Proceedings of the National Academy of Sciences **108**, 15687 (2011).
[20] Y. Wang and et al., Nature **491**, 51 (2012).
[21] N. B. Schade, M. C. Holmes-Cerfon, E. R. Chen, D. Aronzon, J. W. Collins, J. A. Fan, F. Capasso, and V. N. Manoharan, Phys. rev. lett. **110**, 148303 (2013).
[22] J. D. Brodin, E. Auyeung, and C. A. Mirkin, Proceedings of the National Academy of Sciences **112**, 4564 (2015).
[23] See Supplemental Material [url], which includes Refs. [15, 36].
[24] R. A. Fisher, Annals of Eugenics **7**, 355 (1937).
[25] A. Kolmogorov, I. Petrovsky, and N. Piskunov, Bull Uni Moskou Ser Int **A1**, 1 (1937).
[26] In experiments, detachment requires energy input and is facilitated by temperature and UV-light cycling [2], while several other possibilities have been proposed [6, 35].
[27] We tried several criteria; the great majority of clusters with ≥ 2 attached monomers (≥ 3 works as well) in a snapshot do create daughters within a short time window after that snapshot. Conversely, the great majority of daughters are created by "active" parents.
[28] W. Van Saarloos, Physics reports **386**, 29 (2003).
[29] J. D. Murray, "Mathematical biology i: an introduction, vol. 17 of interdisciplinary applied mathematics," (2002).
[30] A. S. Zadorin, Y. Rondelez, J.-C. Galas, and A. Estevez-Torres, Physical Review Letters **114**, 068301 (2015).
[31] I. Bottero, J. Huck, T. Kosikova, and D. Philp, Journal Of The American Chemical Society , jacs.6b03372 (2016).
[32] S. Angioletti-Uberti, P. Varilly, B. M. Mognetti, and D. Frenkel, Physical Review Letters **113**, 128303 (2014).
[33] S. Sahu, P. Yin, and J. H. Reif, in *DNA Computing*, Lecture Notes in Computer Science No. 3892, edited by A. Carbone and N. A. Pierce (Springer Berlin Heidelberg, 2006) pp. 290–304.
[34] D. Yao, T. Song, X. Sun, S. Xiao, F. Huang, and H. Liang, Journal of the American Chemical Society **137**, 14107 (2015).
[35] R. Zhang, J. M. Dempster, and M. Olvera de la Cruz, Soft Matter (2013).
[36] M. Holmes-Cerfon, S. J. Gortler, and M. P. Brenner,

Proceedings of the National Academy of Sciences **110**,
E5 (2013).